



HAL
open science

Influence of an external electric field on the potential-energy surface of alkali-metal-decorated C 60

Deb Sankar De, Santanu Saha, Luigi Genovese, Stefan Goedecker

► **To cite this version:**

Deb Sankar De, Santanu Saha, Luigi Genovese, Stefan Goedecker. Influence of an external electric field on the potential-energy surface of alkali-metal-decorated C 60. *Physical Review A : Atomic, molecular, and optical physics* [1990-2015], 2018, 97 (6), 10.1103/PhysRevA.97.063401 . hal-02141912

HAL Id: hal-02141912

<https://hal.science/hal-02141912>

Submitted on 22 Jul 2024

HAL is a multi-disciplinary open access archive for the deposit and dissemination of scientific research documents, whether they are published or not. The documents may come from teaching and research institutions in France or abroad, or from public or private research centers.

L'archive ouverte pluridisciplinaire **HAL**, est destinée au dépôt et à la diffusion de documents scientifiques de niveau recherche, publiés ou non, émanant des établissements d'enseignement et de recherche français ou étrangers, des laboratoires publics ou privés.

Influence of an external electric field on the potential-energy surface of alkali-metal-decorated C₆₀

Deb Sankar De,¹ Santanu Saha,¹ Luigi Genovese,² and Stefan Goedecker¹
¹*Department of Physics, Universität Basel, Klingelbergstr. 82, 4056 Basel, Switzerland*
²*Univ. Grenoble Alpes, CEA, INAC-SP2M, L_Sim, F-38000, Grenoble, France*



(Received 19 March 2018; published 4 June 2018)

We present a fully *ab initio*, unbiased structure search of the configurational space of decorated C₆₀ fullerenes in the presence of an electric field. We observed that the potential-energy surface is significantly perturbed by an external electric field and that the energetic ordering of low-energy isomers differs with and without electric field. We identify the energetically lowest configuration for a varying number of decorating atoms ($1 \leq n \leq 12$) for Li and ($1 \leq n \leq 6$) for K on the C₆₀ surface at different electric-field strengths. Using the correct geometric ground state in the electric field for the calculation of the dipole we obtain better agreement with the experimentally measured values than previous calculations based on the ground state in absence of an electric field. Since the lowest-energy structures are typically nearly degenerate in energy, a combination of different structures is expected to be found at room temperature. The experimentally measured dipole is therefore also expected to contain significant contributions from several low-energy structures.

DOI: [10.1103/PhysRevA.97.063401](https://doi.org/10.1103/PhysRevA.97.063401)

I. INTRODUCTION

For the past three decades, fullerenes played a prominent role in the field of nanoscience and nanotechnology because of their unusual chemical and physical properties. By doping bulk fullerenes with alkali metals, one can obtain intercalation compounds with interesting physical properties such as superconductivity [1–4]. Alkaline and alkaline-earth-metals coated C₆₀ and carbon nanotubes has been suggested as a potential hydrogen storage material [5–10]. Recently, it has been suggested that applying an electric field vertical to the surface of the metal decorated graphene (or other systems) enhances the hydrogen adsorption [11–14]. Moreover, this process is a reversible process and hydrogen can be easily desorbed by applying an opposite electric field.

Electric dipole measurements provide a convenient way to determine the electronic and geometrical structures of metal decorated C₆₀ [15,16]. Structural changes induced by an electric field have been observed for various systems such as polycrystalline pentacene-based organic transistors [17], pentacene single crystals [18], and polar or nonpolar molecules in a dodecahedral water cage [19]. Uncoated fullerenes are prone to structural changes in the gas phase in the presence of an electric field [20,21].

Rayane *et al.* measured the polarizability and the permanent electric dipole moment of isolated KC₆₀ molecules using molecular-beam deflection [22]. Their results suggested that the polarizability of KC₆₀ is induced by the free skating of the potassium atom on the C₆₀ surface. Antoine *et al.* extended the work to different alkali-metal decorated C₆₀'s [23]. They observed that the dipole moment increases steadily for the elements from top to bottom of the first column of the Periodic Table. A strong charge transfer between a single alkali-metal atom and the C₆₀ cage has been reported resulting in a large electric dipole moment [23,24]. Dugourd *et al.* observed a high electric susceptibility of Na_{*n*}C₆₀ (*n* is the number of Na

atoms) [25]. The results were attributed to a high electric dipole arising from the aggregation of Na_{*n*} on the C₆₀. Antoine *et al.* also measured electric susceptibilities for Li_{*n*}C₆₀ and Na_{*n*}C₆₀ clusters containing up to *n* = 20 alkali-metal atoms [26]. From the experimental data, they concluded that for more than seven Na atoms all atoms aggregate into a single cluster, whereas for Li not all atoms on C₆₀ participate in such a clustering if more than 12 atoms are present.

Antonio *et al.* also explained their experimental results by using a parametrized many-body force field in combination with basin hopping [27] to find the most stable structure for Li and Na decorated C₆₀ [26]. However, the calculated electrostatic dipole moments for the previously known ground states for different *n* did not match with the experimental results. Rabilloud *et al.* computed the dipole moments of C₆₀ structures decorated with a few Li and Na atoms at the DFT level [28]. By comparing the dipole moments with the experimental value, it was suggested that the configurations whose dipole moments are closer to the experimental values might be present in the experiment, even though they are energetically higher than other structures.

In this work we present an unbiased PES scan for Li and K decorated C₆₀ at the DFT level in the presence of an electric field. The wavelet basis set of the BIGDFT code is highly suitable for such a calculation. One can use free boundary conditions which allow for a constant electric field throughout the simulation box. In addition the basis set is systematic and adapts itself fully to the distortion of the wave function induced by the electric field. In this way results of identical high quality can be obtained with and without electric field.

In previous work, we have observed that Li and K atoms prefer to homogeneously distribute over C₆₀ up to 12 and 6 atoms, respectively, in the absence of an external electric field [29]. For this reason we have limited the present PES scan to this maximum number of atoms.

II. METHODS

The unbiased structural prediction of decorated fullerenes in an external electric field was conducted using the minima hopping method [30–32], as implemented in the BIGDFT package [33]. MHM aims to search the global minimum on the potential-energy surface while gradually exploring the other low-energy structures. The efficiency of the MHM method is due to the exploitation of the Bell-Evans-Polanyi principle for molecular dynamics [34]. This method has been successfully applied to many different systems for global geometry optimization [35–43].

The BIGDFT code is a density-functional code using a systematic Daubechies wavelet basis set [44]. The Perdew-Burke-Ernzerhof exchange-correlation functional [45] as implemented in the LibXC library [46] was used together with PBE dual-space Gaussian pseudopotentials with a nonlinear core correction [47–49]. Tight electronic parameters were chosen such that total energy differences were converged to at least 10^{-4} eV for all stable configurations. The forces in geometry relaxations were converged to below $1 \text{ meV}/\text{\AA}$.

III. RESULTS AND DISCUSSION

A. Single Li and K atom on C_{60}

From our previous calculations, we know that alkali-metal atoms, except for Li, prefer to adsorb on the hexagonal site [29]. The potential-energy surface can be altered by applying an external electric field and desired configurations can be stabilized. In the presence of a sufficiently strong electric field, the pentagonal site can however become energetically preferable, as shown in Fig. 1.

Alkali-metal atoms make strong ionic bonds with C_{60} acting as an electron donor for the C_{60} [23,24]. The donated charge is strongly localized on the carbon that is closest to the metal atom. As the strength of the electric field increases, the positively charged alkali-metal atom moves in the direction of the electric field, while the negatively charged C_{60} moves in the

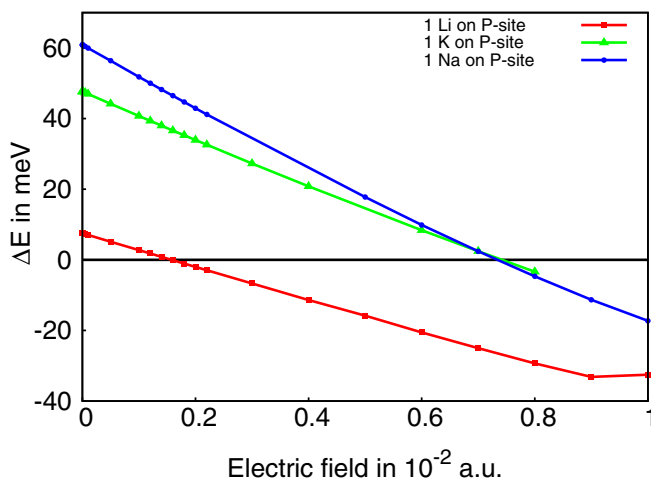


FIG. 1. Energy of the pentagonal site with respect to the hexagonal site for one Li, K, or Na atom on C_{60} as a function of the electric-field strength.

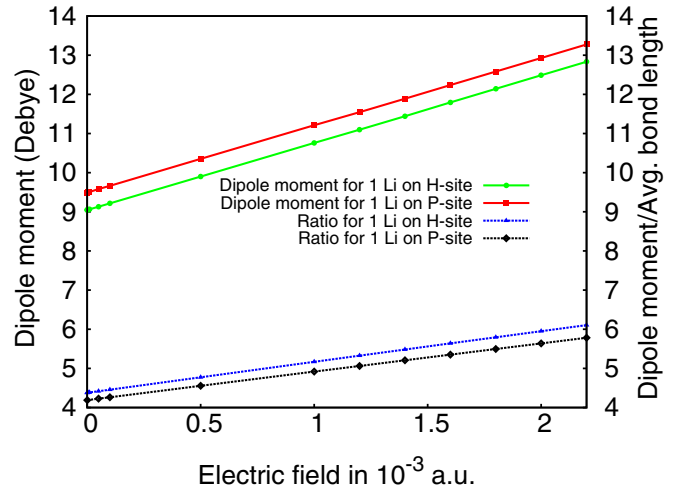


FIG. 2. Dipole moment and the ratio of dipole moment and average bond length between the alkali-metal atom and the carbon atom from the C_{60} vs electric field for one Li atom on the surface of a C_{60} .

opposite direction. This increase in the distance between the positive and negative charge leads to a mainly linear increase of the dipole moment with respect to the field strength since the charges remain more or less constant as shown in Fig. 2.

B. Li and K on the fullerene surface

In this section, we provide further insight into the behavior of C_{60} 's decorated with more than one Li in the presence of an electric field. The number of atoms on the C_{60} surface is stepwise increased from 2 to 12 for Li and from 2 to 6 for K. The electric field used for these calculations was 5×10^{-5} atomic unit (a.u.), which is comparable to the strength of the experimentally applied electric field ($7 \times 10^2 \text{ V/m}$) [26]. We also performed another MH run with an electric field of 1×10^{-3} a.u., which corresponds to a strong experimental field reached for instance in the tip of a scanning microscope [50]. We started our calculations with the lowest-energy structure at zero electric field. Figure 3 presents two energetically quasidegenerate metastable structures in the absence of an electric field. In one structure, one of the two Li atoms is on P site [Fig. 3(a)], whereas both Li atoms are on H site in the other structure [Fig. 3(b)]. At low electric field (5×10^{-5} a.u.) they are still energetically degenerate. As we increase the electric field, the energy difference between these structures increases

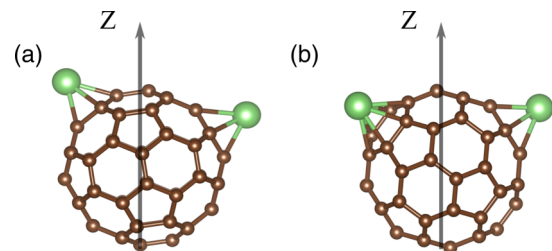


FIG. 3. Two isomers [(a) and (b)] found for an electric field of 5×10^{-5} a.u. The electric field is along the Z direction.

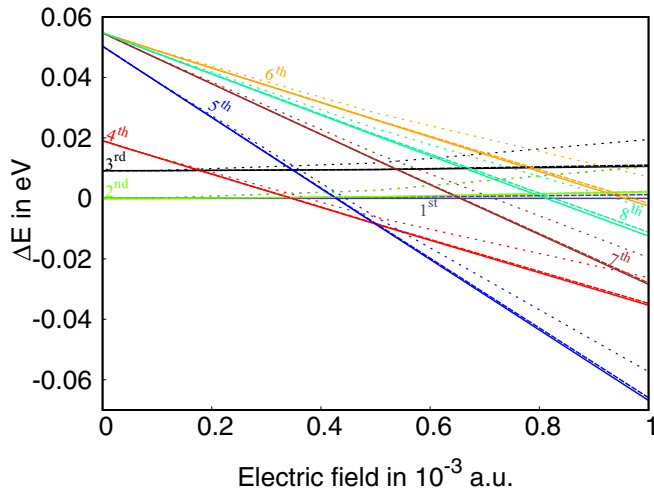


FIG. 4. Solid lines show the energy of eight isomers of Li_2C_{60} as a function of the applied electric field, whereas the dotted lines show their energies obtained from the first-order perturbation theory and the dashed lines give their energies obtained from the second-order perturbation theory. All energies are calculated with respect to the lowest-energy structure at zero electric field. The dashed lines overlap with the solid lines. The numbering of the structures in the plot corresponds to the energy ordering of the structures at zero electric field. First and second structure is energetically the same at the low electric fields.

strongly (fourth and fifth lowest-energy structure of Fig. 4). A similar situation arises for more than two Li atoms.

To establish the energetic ordering of the structures as a function of the field strength, we relaxed the 20 lowest-energy structures from minima hopping runs at different electric-field strengths and the first eight of them are plotted in Fig. 4. The two structures that were initially the lowest-energy structures are not any more energetically favorable at a strength of 4×10^{-4} a.u., while other structures are lowered in energy. Different energetic orderings at different electric fields are also observed for more than 2 Li atoms on the C_{60} surface. In addition to the total energies E_{tot} calculated consistently in the electric field, we have plotted in Fig. 4 also the energies from first- and second-order perturbation theory, which are given by

$$E = E(\mathcal{E} = 0) - \sum_i P_i \mathcal{E}_i - \frac{1}{2} \sum_i \sum_j \alpha_{ij} \mathcal{E}_i \mathcal{E}_j, \quad (1)$$

where \mathcal{E} is the applied electric field, P_i and α_{ij} are the static dipole moment and polarizability, respectively, and $E(\mathcal{E} = 0)$ is the energy of the system without electric field. At low electric field the dotted and solid lines overlap, but at higher electric-field strengths they deviate, showing that first-order perturbation theory cannot predict the correct energetic ordering for strong experimental fields. This is because the change in dipole moment is not considered. As we add the second-order perturbation term to the energy, the energies almost overlap with the actual energy. This shows that the second-order variation in energy due to the first-order variation of the dipole moment (i.e., linear polarizability term) is necessary for an accurate description of this system in the strong electric fields.

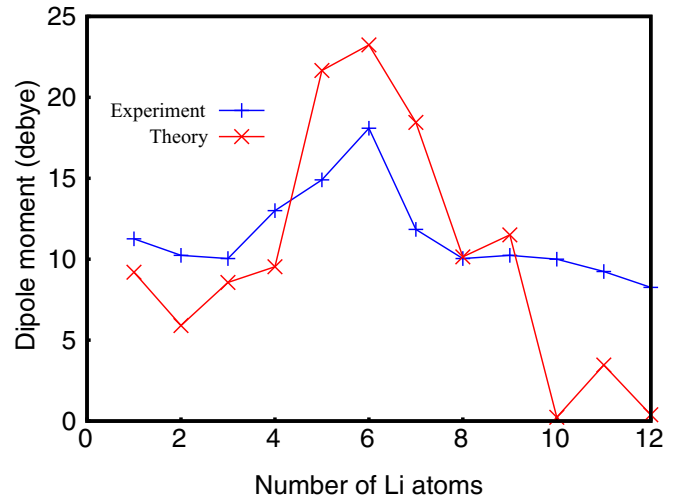


FIG. 5. Theoretical and experimental [26] dipole moments for the lowest-energy structure for different number of Li atoms decorated C_{60} . The experimental data is obtained from the article by Antonio *et al.* [26]. For theoretical calculation, the applied electric field is 5×10^{-5} a.u. and, for experiment, 3×10^{-5} a.u.

The dipole moments for different numbers of Li atoms are plotted in Fig. 5 for a field strength of 5×10^{-5} a.u. The experimental values [26] are intrinsically Boltzmann averages over low-energy configurations, whereas the theoretical value is only obtained from the lowest-energy configuration, because it would be computationally too expensive to calculate the energies of a large number of structures for many different field strengths. If there is an energetically degenerate state for a particular number of Li atoms, we have taken the one with the highest dipole moment. In contrast to the experimental results which were obtained at room temperature, our results are at zero temperature, since it would also be computationally too expensive to calculate the required large number of free energies. In spite of these differences between the experimental and theoretical dipole moments, Fig. 5 shows similar trends such as a peak of the dipole moment for six Li atoms.

In order to study the stability of some selected configurations at finite temperature, we calculated free energies. We calculated in the standard way [51] the vibrational frequencies ω_i and the zero point energy E_{ZP} to obtain the free energy F ,

$$F = E_0 - E_{\text{ZP}} + k_B T \sum_i \ln \left[\exp \left(\frac{\hbar \omega_i}{k_B T} \right) - 1 \right]. \quad (2)$$

Figure 6 shows that the lowest-energy structure at zero temperature is still the lowest in energy at room temperature and remains highly populated. There is, however, a high probability of populating the higher-energy structures (Fig. 7). The dipole moment for fifth and sixth configuration is quite high (~ 10 Debye). These structures will be present during the measurement of dipole moment at room temperature and contribute to the total dipole moment. In Fig. 8, we have calculated the total dipole moment as a sum of the dipole moments of different structures weighted by their Boltzmann probability factors. As we include more isomers the total dipole moment tends towards the experimental value (10.2 Debye) at room temperature. Reproducing exactly the experimental value is,

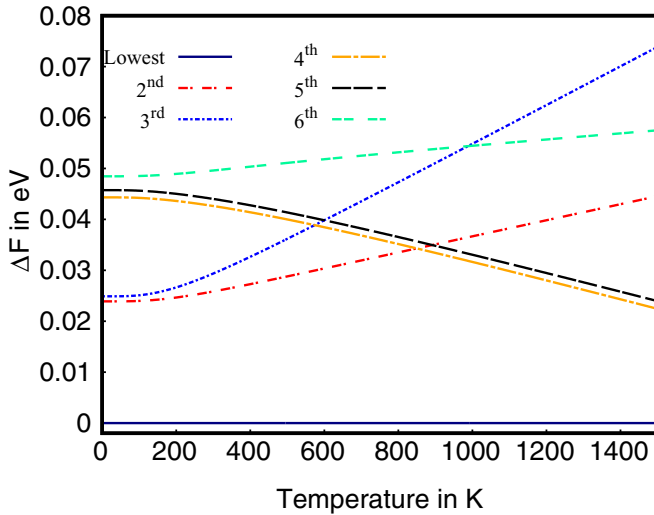


FIG. 6. Free energy for the six lowest-energy configurations. The free energies are plotted with respect to the energy of the lowest-energy configuration at 0 K. The applied electric field is 5×10^{-5} a.u.

however, elusive since the intrinsic errors of density-functional theory are larger than $k_B T$ at room temperature and hence it is not possible to obtain reliable Boltzmann probabilities.

C_{60} does not have double bonds within the pentagonal rings. Hence one electron is missing to obtain an additional stabilization by aromaticity. As a result, C_{60} behaves like an electron deficient alkene and readily reacts with electron rich species. The estimated electron affinity and ionization potential values for C_{60} are 2.7 eV and 7.8 eV, respectively [52]. The neutral C_{60} can take six extra electron to achieve higher aromaticity. Even an additional six electrons can be accommodated [53]. Such a C_{60}^{n-} (where $n = 2, 3, 4$) structure is short lived [54,55], but can be stabilized by an Li^+ [28,56]. This explains the experimentally observed [57] and theoretically confirmed [29] homogeneous absorption of up to 12 Li atoms on C_{60} . Hence,

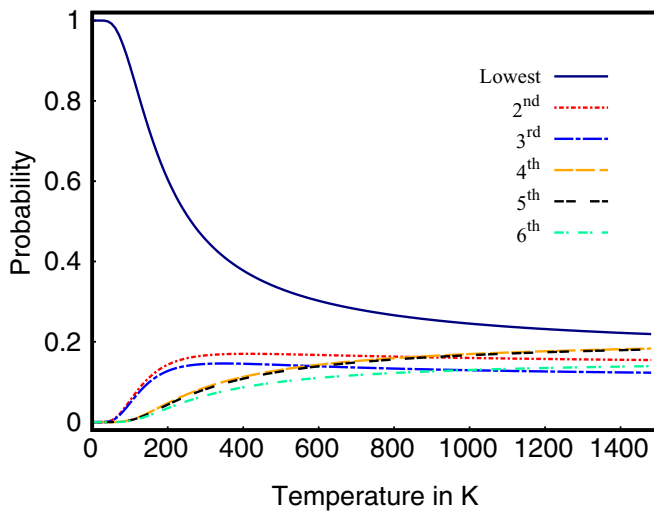


FIG. 7. Normalized Boltzmann factors as a function of temperature for the six low-energy configurations. The applied electric field is 5×10^{-5} a.u.

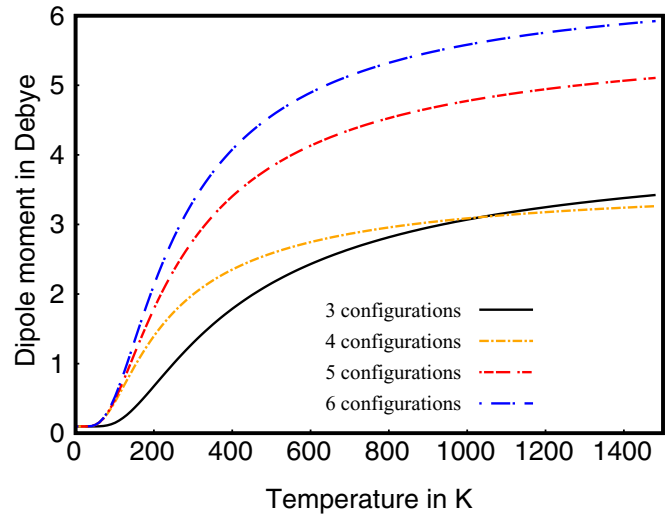


FIG. 8. Dipole moment of the system at different temperatures obtained by weighting the dipole of the individual structures by their Boltzmann factor. The applied electric field is 5×10^{-5} a.u.

to alter this distribution pattern, a high electric field is required. The configurations that are provided in our previous work [29] are the most stable configurations up to a field strength of 1×10^{-3} a.u. for Li_4 and 3×10^{-3} a.u. for Li_6 and Li_{11} . For even stronger fields the Li atoms are detached from the C_{60} , but clustering is never observed.

The PES of the K atom decorated C_{60} slowly changes with an increasing electric field. Table II contains the energy ordering for the first 10 lowest-energy structures of K_2C_{60} at different electric fields. The lowest-energy structure which is observed at very low electric field is different from the lowest-energy structure in the absence of an electric field. As the number of K atom is increased, the structures are even more stable and require high electric field to alter the energy ordering, for example, for K_6C_{60} and the PES alters at the electric field of 1×10^{-3} a.u.

In Table I, we have shown the dipole moment of the lowest-energy structures of K decorated C_{60} at the electric field of 5×10^{-5} a.u. Our calculated dipole moment for one K atom on C_{60} is 15 Debye in an electric field of 5×10^{-5} a.u. The ATD profile with an electric field of 1.5×10^7 V/m is in good agreement with the profile simulated for a permanent (and rigid) dipole moment of 17.7 Debye, which is very close to the theoretical value [22,24]. If we increase the number of K atoms, many energetically degenerate structures appear as we increase the applied electric field (Table II). We have not

TABLE I. Dipole moment of the lowest-energy structure for different number of K atoms decorated C_{60} . The applied electric field is 5×10^{-5} a.u.

Number of K atoms	1	2	3	4	5	6
Dipole moment (Debye)	15.38	10.19	5.73	0.35	11.09	0.21

TABLE II. Energy of the first 10 K_2C_{60} structures at different electric field. The energies are given with respect to the lowest-energy structure at that particular electric field in eV.

Structure ordering	5×10^{-5} a.u.	1×10^{-4} a.u.	5×10^{-4} a.u.	1×10^{-3} a.u.
1	0.000	0.037	0.055	0.096
2	0.009	0.074	0.000	0.000
3	0.019	0.097	0.107	0.221
4	0.021	0.104	0.139	0.289
5	0.068	0.000	0.106	0.028
6	0.068	0.000	0.107	0.026
7	0.072	0.095	0.113	0.127
8	0.088	0.164	0.158	0.252
9	0.119	0.201	0.263	0.438
10	0.138	0.201	0.179	0.208

found the experimental dipole moment for C_{60} with more than one K atom in the literature.

We also investigated if all C_{60} molecules in a group will have exactly the same number of K atoms on the surface or whether there may be a redistribution of decorating K atoms on C_{60} molecules. We checked, for example, whether two K_4C_{60} are energetically more favorable than one K_3C_{60} and one K_5C_{60} . We calculated the energy difference for those two cases using the following equation:

$$E_{\text{diff}} = 2 \times E_{K_4C_{60}} - E_{K_3C_{60}} - E_{K_5C_{60}}. \quad (3)$$

We found a tiny energy difference (E_{diff}) of 0.14 eV, which indicates that they are energetically degenerate. Hence two K_4C_{60} structures are equally likely to occur than one K_3C_{60}

and one K_5C_{60} . Experimentally, however, it is possible to obtain a group of C_{60} atoms with an identical number of K atoms [22,23,26].

IV. CONCLUSIONS

We have explored the PES of Li and K decorated C_{60} in the presence of electric fields of varying strength by an unbiased search method at the DFT level. The experimental field strengths, that can for instance be obtained near the tip in a scanning microscope, induce considerable changes of the PES and alter the energetic ordering of C_{60} isomers decorated with a small number of metal atoms. Some structures which are metastable in the absence of an electric field can become ground states by varying the strength of the electric field. In this way one can switch between two structures by increasing or weakening the electric field. A correct calculation of measured dipoles requires one to use all those configurations which are the lowest in energy at the given electric field. Since these configurations are frequently virtually degenerate in energy, several configurations can make significant contributions to the dipole moment. Accurate results in strong experimental fields cannot be obtained by perturbation theory but require a fully self-consistent electronic structure calculation for the given field strength.

ACKNOWLEDGMENTS

D.S.D. acknowledges support from the Swiss National Science Foundation-SNF. Computing resources were provided by the CSCS in Lugano under Project No. s707. Calculations were also performed at the sciCORE [58] scientific computing core facility at the University of Basel. This work was done partially within the NCCR MARVEL project.

- [1] O. Gunnarsson, *Rev. Mod. Phys.* **69**, 575 (1997).
- [2] M. Mitrano, A. Cantaluppi, D. Nicoletti, S. Kaiser, A. Perucchi, S. Lupi, P. Di Pietro, D. Pontiroli, M. Riccò, S. R. Clark *et al.*, *Nature (London)* **530**, 461 (2016).
- [3] H. Takeya, T. Konno, C. Hirata, T. Wakahara, K. Miyazawa, T. Yamaguchi, M. Tanaka, and Y. Takano, *J. Phys.: Condens. Matter* **28**, 354003 (2016).
- [4] M. Kim, Y. Nomura, M. Ferrero, P. Seth, O. Parcollet, and A. Georges, *Phys. Rev. B* **94**, 155152 (2016).
- [5] T. Yildirim, J. Íñiguez, and S. Ciraci, *Phys. Rev. B* **72**, 153403 (2005).
- [6] K. Chandrakumar and S. K. Ghosh, *Nano Lett.* **8**, 13 (2008).
- [7] M. Yoon, S. Yang, C. Hicke, E. Wang, D. Geohegan, and Z. Zhang, *Phys. Rev. Lett.* **100**, 206806 (2008).
- [8] Q. Wang, Q. Sun, P. Jena, and Y. Kawazoe, *J. Chem. Theory Comput.* **5**, 374 (2009).
- [9] H. Lee, J. Ihm, M. L. Cohen, and S. G. Louie, *Phys. Rev. B* **80**, 115412 (2009).
- [10] A. Kaiser, M. Renzler, L. Kranabetter, M. Schwärzler, R. Parajuli, O. Echt, and P. Scheier, *Int. J. Hydrogen Energy* **42**, 3078 (2017).
- [11] X. Zhang, C. Tang, and Q. Jiang, *Int. J. Hydrogen Energy* **41**, 10776 (2016).
- [12] W. Liu, Y. Zhao, J. Nguyen, Y. Li, Q. Jiang, and E. Lavernia, *Carbon* **47**, 3452 (2009).
- [13] S. Shi, J.-Y. Hwang, X. Li, X. Sun, and B. I. Lee, *Int. J. Hydrogen Energy* **35**, 629 (2010).
- [14] E. H. Song, S. H. Yoo, J. J. Kim, S. W. Lai, Q. Jiang, and S. O. Cho, *Phys. Chem. Chem. Phys.* **16**, 23985 (2014).
- [15] M. Broyer, R. Antoine, E. Benichou, I. Compagnon, P. Dugourd, and D. Rayane, *C. R. Phys.* **3**, 301 (2002).
- [16] P. Dugourd, R. Antoine, G. Breaux, M. Broyer, and M. F. Jarrold, *J. Am. Chem. Soc.* **127**, 4675 (2005).
- [17] H.-L. Cheng, W.-Y. Chou, C. Kuo, F.-C. Tang, and Y.-W. Wang, *Appl. Phys. Lett.* **88**, 161918 (2006).
- [18] K. Kotsuki, S. Obata, and K. Saiki, *Langmuir* **30**, 14286 (2014).
- [19] N. D. Gurav, S. P. Gejji, L. J. Bartolotti, and R. K. Pathak, *J. Chem. Phys.* **145**, 074302 (2016).
- [20] H. Shen, *Int. J. Nanosci.* **4**, 389 (2005).
- [21] J.-y. Sorimachi and S. Okada, *Chem. Phys. Lett.* **659**, 1 (2016).
- [22] D. Rayane, R. Antoine, Ph. Dugourd, E. Benichou, A. R. Allouche, M. Aubert-Frécon, and M. Broyer, *Phys. Rev. Lett.* **84**, 1962 (2000).

- [23] R. Antoine, D. Rayane, E. Benichou, P. Dugourd, and M. Broyer, *Eur. Phys. J. D* **12**, 147 (2000).
- [24] F. Rabilloud, *Comput. Theor. Chem.* **964**, 213 (2011).
- [25] P. Dugourd, R. Antoine, D. Rayane, I. Compagnon, and M. Broyer, *J. Chem. Phys.* **114**, 1970 (2001).
- [26] F. Rabilloud, R. Antoine, M. Broyer, I. Compagnon, P. Dugourd, D. Rayane, F. Calvo, and F. Spiegelman, *J. Phys. Chem. C* **111**, 17795 (2007).
- [27] J. P. K. Doye and D. J. Wales, *Phys. Rev. Lett.* **80**, 1357 (1998).
- [28] F. Rabilloud, *J. Phys. Chem. A* **114**, 7241 (2010).
- [29] D. S. De, J. A. Flores-Livas, S. Saha, L. Genovese, and S. Goedecker, *Carbon* **129**, 847 (2018).
- [30] S. Goedecker, *J. Chem. Phys.* **120**, 9911 (2004).
- [31] B. Schaefer, S. Alireza Ghasemi, S. Roy, and S. Goedecker, *J. Chem. Phys.* **142**, 034112 (2015).
- [32] S. Goedecker, W. Hellmann, and T. Lenosky, *Phys. Rev. Lett.* **95**, 055501 (2005).
- [33] L. Genovese, A. Neelov, S. Goedecker, T. Deutsch, S. A. Ghasemi, A. Willand, D. Caliste, O. Zilberberg, M. Rayson, A. Bergman, and R. Schneider, *J. Chem. Phys.* **129**, 014109 (2008).
- [34] S. Roy, S. Goedecker, and V. Hellmann, *Phys. Rev. E* **77**, 056707 (2008).
- [35] M. Amsler, J. A. Flores-Livas, L. Lehtovaara, F. Balima, S. A. Ghasemi, D. Machon, S. Pailhes, A. Willand, D. Caliste, S. Botti *et al.*, *Phys. Rev. Lett.* **108**, 065501 (2012).
- [36] M. Amsler, J. A. Flores-Livas, T. D. Huan, S. Botti, M. A. L. Marques, and S. Goedecker, *Phys. Rev. Lett.* **108**, 205505 (2012).
- [37] S. Botti, J. A. Flores-Livas, M. Amsler, S. Goedecker, and M. A. L. Marques, *Phys. Rev. B* **86**, 121204(R) (2012).
- [38] S. Botti, M. Amsler, J. A. Flores-Livas, P. Ceria, S. Goedecker, and M. A. L. Marques, *Phys. Rev. B* **88**, 014102 (2013).
- [39] J. A. Flores-Livas, A. Sanna, and E. Gross, *Eur. Phys. J. B* **89**, 63 (2016).
- [40] M. Amsler, J. A. Flores-Livas, M. A. Marques, S. Botti, and S. Goedecker, *Eur. Phys. J. B* **86**, 383 (2013).
- [41] B. Schaefer, R. Pal, N. S. Khatri, M. Amsler, A. Sadeghi, V. Blum, X. C. Zeng, S. Goedecker, and L.-S. Wang, *ACS Nano* **8**, 7413 (2014).
- [42] J. A. Flores-Livas, M. Amsler, T. J. Lenosky, L. Lehtovaara, S. Botti, M. A. L. Marques, and S. Goedecker, *Phys. Rev. Lett.* **108**, 117004 (2012).
- [43] J. A. Flores-Livas, M. Amsler, C. Heil, A. Sanna, L. Boeri, G. Profeta, C. Wolverton, S. Goedecker, and E. K. U. Gross, *Phys. Rev. B* **93**, 020508(R) (2016).
- [44] I. Daubechies, *Ten Lectures on Wavelets* (SIAM, Philadelphia, 1992), Vol. 61.
- [45] J. P. Perdew, K. Burke, and M. Ernzerhof, *Phys. Rev. Lett.* **77**, 3865 (1996).
- [46] M. A. Marques, M. J. Oliveira, and T. Burnus, *Comput. Phys. Commun.* **183**, 2272 (2012).
- [47] S. Goedecker, M. Teter, and J. Hutter, *Phys. Rev. B* **54**, 1703 (1996).
- [48] A. Willand, Y. O. Kvashnin, L. Genovese, A. Vazquez Mayagoitia, A. K. Deb, A. Sadeghi, T. Deutsch, and S. Goedecker, *J. Chem. Phys.* **138**, 104109 (2013).
- [49] C. Hartwigsen, S. Goedecker, and J. Hutter, *Phys. Rev. B* **58**, 3641 (1998).
- [50] J. A. Stroschio and D. Eigler, *Science* **254**, 1319 (1991).
- [51] J. Ochterski, *Thermochemistry in Gaussian* (Gaussian, Wallingford, CT, 2000).
- [52] A. Rosén and B. Wästberg, *J. Chem. Phys.* **90**, 2525 (1989).
- [53] K. E. Geckeler, *Advanced Macromolecular and Supramolecular Materials and Processes* (Springer, Berlin, 2003).
- [54] V. Cammarata, T. Guo, A. Illies, L. Li, and P. Shevlin, *J. Phys. Chem. A* **109**, 2765 (2005).
- [55] S. Tomita, J. U. Andersen, H. Cederquist, B. Concina, O. Echt, J. Forster, K. Hansen, B. Huber, P. Hvelplund, J. Jensen *et al.*, *J. Chem. Phys.* **124**, 024310 (2006).
- [56] C. Yannouleas and U. Landman, *Chem. Phys. Lett.* **217**, 175 (1994).
- [57] U. Zimmermann, N. Malinowski, A. Burkhardt, and T. Martin, *Carbon* **33**, 995 (1995).
- [58] <http://scicore.unibas.ch/>.